agronomy

MDPI

Article

Three Cycles of Continuous Propagation of a Severe PSTVd Strain NicTr-3 in *Solanum lycopersicum* cv. Rutgers Resulted in Its Attenuation and Very Mild Disease Symptoms in Potato

Alex V. Kochetov [1,2,3,*], Nikolay Shmakov [1,2], Dmitry A. Afonnikov [1,2], Gennady V. Vasiliev [1], Natalja V. Shatskaya [1], Anastasiya A. Egorova [1], Nina V. Mironenko [4], Nina M. Lashina [4], Alexander V. Khiutti [4] and Olga S. Afanasenko [4]

[1] Institute of Cytology & Genetics, Novosibirsk 630090, Russia
[2] Faculty of Natural Sciences, Novosibirsk State University, Novosibirsk 630090, Russia
[3] Faculty of Agronomy, Novosibirsk State Agrarian University, Novosibirsk 630039, Russia
[4] All Russian Institute of Plant Protection, St.-Petersburg 196608, Russia
* Correspondence: ak@bionet.nsc.ru

Abstract: Potato spindle tuber viroid (PSTVd) is a small infectious non-coding circular RNA causing diseases of important crops, including tomato and potato. The symptoms vary from mild to severe depending on the viroid strain, the host plant variety, and the environmental conditions. The molecular mechanisms underlying the development of particular disease phenotypes remain elusive. The PSTVd strain NicTr-3 causes severe disease symptoms on Solanum lycopersicum cv. Rutgers and Solanum tuberosum cv. Colomba. It was found that after three cycles of propagation in tomato cv. Rutgers, infection of potato cv. Colomba with NicTr-3 resulted in very mild symptoms including smaller size of tubers and delayed leaf senescence. Sequence analysis of PSTVd clones isolated from tomato inoculum revealed the presence of mutated variants of genomic RNA. Transcriptome analysis carried out on leaves showed a considerable difference between infected and healthy plants at 14 dpi and 30 dpi. Interestingly, the response of potato plants to the attenuated PSTVd strain revealed a large number of DEGs associated with initiation of dormancy with a considerable increase in the vegetation period. The second vegetative generation (tuber-derived plantlets from control healthy and PSTVd-infected plants) was characterized by similar phenotypes and transcriptomes. Thus, here we describe a case of attenuation of a severe PSTVd strain after continuous propagation in tomato. It would be of interest to consider the attenuated viroid strains as a potential biocontrol agent or vaccine against this type of pathogenic RNA.

Keywords: viroid; PSTDv; attenuation; potato; dormancy

Citation: Kochetov, A.V.; Shmakov, N.; Afonnikov, D.A.; Vasiliev, G.V.; Shatskaya, N.V.; Egorova, A.A.; Mironenko, N.V.; Lashina, N.M.; Khiutti, A.V.; Afanasenko, O.S. Three Cycles of Continuous Propagation of a Severe PSTVd Strain NicTr-3 in *Solanum lycopersicum* cv. Rutgers Resulted in Its Attenuation and Very Mild Disease Symptoms in Potato. *Agronomy* **2023**, *13*, 684. https://doi.org/10.3390/agronomy13030684

Academic Editor: Richard G. F. Visser

Received: 15 January 2023
Revised: 14 February 2023
Accepted: 20 February 2023
Published: 26 February 2023

1. Introduction

Potato spindle tuber viroid (PSTVd) is a member of the Pospiviroid genus in the viroid family Pospiviridae [1]. PSTVd infects several solanaceous crops causing serious diseases in tomato (*Solanum lycopersicum*) and potato (*S. tuberosum*), and to a lesser extent in pepper and chili (*Capsicum annuum*). It may infect pepino (*S. muricatum*) in natural populations without symptoms [2]. The pathogen has quarantine status and is registered on all continents according to the European Plant Protection Organization [3].

It has been shown that tomato strains of PSTVd can be highly pathogenic for representatives of widely used potato cultivars [4,5]. The aggressiveness of PSTVd strains (mild, intermediate, or severe) is commonly evaluated on the highly susceptible host tomato cultivar Rutgers [6,7]. PSTVd infection may cause disease symptoms in potato plants including stunting, shortening internodes and petioles, and epinasty and wrinkling of leaves. Tubers are elongated and become small and deformed upon infection.

The mechanisms underlying the development of disease symptoms are still under investigation. Viroid circular RNA is not protein-coding and its replication is mediated through host cellular machinery. It is known that the disease symptoms vary and may depend on the PSTVd strain, host genotype, and environmental conditions [8]. Comparison between mild and severe viroid isolates revealed a number of mutations in their RNAs associated with different disease phenotypes of tomato cv. Rutgers [9]. Indeed, viroid RNA is prone to mutations during the replication process and may be represented in the plant by a number of variants (quasi-species) [10]. In turn, host influence may be illustrated by tomato cultivars Rutgers and Moneymaker with severe and very mild symptoms of PSTVd infection, respectively [11]. Some wild tomato species have been characterized with tolerance to the lethal PSTVd strains, and this trait can be inherited in hybrids with susceptible species [12].

It is considered that RNA interference resulting from RNA–RNA interactions may be the cause of the disease phenotype through suppression of host target genes. It has been demonstrated that PSTVd-derived small RNAs can target several genes, including three serine threonine kinase receptors [13]. In potato, viroid-derived small RNAs were associated with the silencing of transcription factor StTCP23, which plays an important role in plant growth and development as well as in hormonal regulation, especially in responses to gibberellic acid. A 21-nt long segment in 3′-UTR of StTCP23 possesses complementarity with the virulence-modulating region (VMR) of PSTVd strain RG1 [14]. Expression of artificial microRNAs with this segment in potato plants resulted in a decrease in expression of the GA biosynthesis-associated genes StGA3ox2, StGA20ox1 and StGA7ox, and upregulation of the GA degrading gene StGA2ox1 [14]. Another study demonstrated a link between PSTVd symptoms severity and the silencing of the sterol glycosyltransferase 1 gene in tomato [15]. Citrus exocortis viroid induced disease symptoms in tomato resulting from the disturbance of translation machinery and ethylene signaling [16].

Despite the experimental evidence of the involvement of viroid-derived small RNAs (vd-sRNAs) in the disease phenotype, this mechanism is hardly common for different viroid-host pathosystems. Computational prediction revealed about one hundred potential mRNA targets for vd-sRNAs in tomato and *Nicotiana benthamiana* transcriptomes, but systemic analysis of degradomes of PSTVd-infected plants revealed only a few suppressed mRNAs from this set with no overlaps between them in different plant species, despite similar disease symptoms [17].

Here, we report the case of attenuation of a severe PSTVd strain NicTr-3 after three cycles of continuous propagation in tomato cv. Rutgers. Infection of potato cv. Colomba resulted in very mild symptoms including smaller size of tubers and delayed leaf senescence. The transcriptome analysis revealed a considerable difference between the leaves of infected and healthy plants resembling the initiation of a dormant state. Interestingly, the tuber-derived plantlets from healthy and infected potato plants were very similar phenotypically and at the transcriptome level.

2. Materials and Methods

2.1. Plant Materials

Tubers of the Netherlands potato cultivar Colomba, super elite category, were obtained from the seed farm agricultural consumer supply and marketing cooperative "Ustyuzhenskiy potato" (Vologda region, RF).

2.2. Resistance Assessment

The PSTVd strain NicTr-3 was isolated from severely affected potato plants of cv. Nikulinskiy from the Novosibirsk Region in 2021 (annotated in GenBank, AC = LC654171). This PSTVd strain causes severe symptoms on tomato cv. Rutgers, including stunting, severe leaf curling, epinasty, and stem and leaf necrosis (Figure 1). RNA of the NicTr-3 strain was synthesized in vitro from plasmid, used for inoculation of tomato cv. Rutgers

plants, and further propagated in tomato plants before the experiment (three cycles of propagation, each with a duration of three months).

(**A**) (**B**) (**C**)

Figure 1. (**A**,**B**)—symptoms on cv. Rutgers tomatoes infected with the PSTVd strain NicTr-3 at 30 days post inoculation (dpi); (**C**)—mock.

Potato plants of cv. Colomba and tomato plants of cv. Rutgers were grown at a temperature of 25 ± 2 °C with a photoperiod of 16 h of light and 8 h of dark under Phytolamps (TL-FITO L1517 88 VR, LED Brand: OSRAM OSLON® SSL) and adequately watered. Each tuber was planted in a 2000 cm^3 plastic pot filled with "Terra vita" soil. Seven-day-old potato plants and 14-day-old tomato plants were used for inoculation with PSTVd.

To prepare the inoculum, 0.1 g of fresh tomato leaf tissue of cv. Rutgers (60 days post inoculation (dpi)) with the PSTVd strain NicTr-3 was ground in 1 mL sodium phosphate buffer (pH 7.0) and filtered through cheesecloth. To inoculate 7-day-old potato plants of cv. Colomba, a 0.5–1.0 cm longitudinal stem incision was performed with a sterile razor on the stem apex and 10 µL of the PSTVd strain suspension was applied. Three plants of cv. Colomba were inoculated and the presence of PSTVd in the inoculated plants was determined using RT-PCR at 14 dpi (stage II—vegetative growth) and 30 dpi (stage III—tuber initiation). Three control plants were mock inoculated with sterile water. The samples from the leaves of the control and infected plants were isolated just before inoculation, at 14 dpi, at 30 dpi, and stored at −80 °C. After 90 days, the presence of tuber deformation, their number, and their weight were evaluated.

2.3. Detection of PSTVd in Potato and Tomato Plants by RT-PCR

Prior to inoculation of potato plants, the presence of viroid RNA in PSTVd-infected tomato plants of cv. Rutgers was evaluated by RT-PCR. Detection of viroid infection was performed in samples taken for transcriptome analysis from each plant before infection and at 14, 30, 60 dpi, as well as in control plants. RNA from potato top leaves was extracted from 0.1 g of leaf tissue using the RNeasy Plant Mini kit (Qiagen, Hilden, Germany) according to the manufacturer's instructions. Detection of PSTVd with primer sets P3/P4 was performed using the Potato spindle tuber viroid-RT kit (Syntol, Moscow, cat. no. PV-004) according to the kit manufacturer's recommendations. RT-PCR was conducted on a MyCycler Thermal Cycler (Bio Rad, Hercules, CA, USA) at 50 °C for 30 min, 94 °C for 2 min, followed by 35 cycles at 94 °C for 30 s, 60 °C for 30 s, and 72 °C for 30 s. An additional synthesis step was performed at 72 °C for 5 min followed by storage at 12 °C. The size of the PSTVd diagnostic fragment was about 360 bp. For each reaction, three technical replicates were run.

2.4. RNA-Seq

Total RNA was extracted with the LRU-100-50 Kit (Biolabmix, Novosibirsk, Russia). The quality of the RNA samples was evaluated using a Bioanalyzer 2100 (Agilent). All

samples had a RIN 7.8 or higher. RNAseq library preparations were carried out with 1 µg of the total RNA fraction using the TruSeq Stranded Plant RNA Library Prep Kit and TruSeq RNA CD Index Plate (Illumina, San Diego, CA, USA) according to the manufacturer's instructions for barcoded libraries with small modifications (6 min RNA fragmentation time and 12 PCR cycles were used). Final libraries quantification was performed with a Bioanalyzer 2100 and the DNA High Sensitivity Kit (Agilent). After normalization, barcoded libraries were pooled and sequenced on a NextSeq 550 sequencer 2 × 75 bp using NextSeq® 500/550 High Output v2.5 Kit 150 cycles (Illumina). Raw sequencing data were deposited in the NCBI Sequence Read Archive (PRJNA914898).

2.5. RT-qPCR

RNA samples were treated with DNAse I (Thermo Fisher Scientific Inc., Waltham, MA, USA). To prepare single-stranded cDNA by reverse transcription, 1 µg aliquots of total RNA samples were used with the RNAscribe RT Plus kit (Biolabmix, Novosibirsk, Russia). Primers for qRT-PCR were designed using the IDT PrimerQuest software (http://eu.idtdna.com/PrimerQuest/Home/; accessed on 2 December 2022) and Primer3 software (https://libnano.github.io/primer3-py/; accessed on 2 December 2022). The EF-Tu gene was used as a reference (accession no. PGSC0003DMG400002992). Transcripts of several differentially expressed genes were selected from the transcriptomic data for qRT-PCR verification. The accession numbers of genes and structures of primers are given in Table S1. The relative expression levels were quantified using the LightCycler® 96 ("Roche") Real Time PCR System. The qPCR was conducted using the HS-qPCR SYBR Blue kit (Biolabmix, Novosibirsk, Russia). For each reaction, three technical replicates were run (Figure S1).

2.6. Bioinformatic Analysis

Bioinformatic analysis was performed for fifteen libraries of mRNA short reads, sequenced on Illumina NextSeq 550. Libraries were sequenced from two organs: leaves (9 libraries) and tuber-derived plantlets (second vegetative generation, 6 libraries). The samples of nucleotide sequences were filtered with FastP version 0.20.1 software [18]. Reads shorter than 50 nucleotides, with a mean Phred quality score less than 20, or containing more than 10% of undefined nucleotides ('N') were removed.

Mapping. Reads of the filtered mRNA libraries were mapped to *S. tuberosum* reference genome version SolTub_3.0 [19]. The genome sequence was downloaded from the Ensembl Plants database [20]. Bwt_index tool was implemented to index the genome sequence, and Dart software version 1.4.6 [21] was used to map the reads to the reference genome.

Expression analysis. The number of reads from the mRNA libraries mapped to the *S. tuberosum* genes was identified with FeatureCounts version 2.0.1 tool from the SubRead package [22]. Potato genome annotation in gff3 format was downloaded from the Ensembl Plants database, version 53. The resulting expression matrix was processed with the EdgeR package [23] version 3.40.0 for R programming language version 4.2.2. The PlotMDS function was used to assess library clustering and define outliers. Enrichment analysis of gene ontology terms was performed for differentially expressed genes (DEGs) using the online service SEA at the AgriGOv2 database [24].

3. Results

3.1. Assessment of Resistance to PSTVd

Recent analysis of modern potato cultivars for resistance against four PSTVd strains has demonstrated that infection with NicTr-3 resulted in tuber malformation in 13 cultivars, including Colomba, as well as in severe disease symptoms in the folia part of PSTVd-infected tuber-derived plantlets of the next generation (Figure S2; [5]). It should be noted that, in that study the NicTr-3 viroid RNA was synthesized in vitro from a synthetic DNA construct and used for inoculation of tomato cv. Rutgers plants, and sap from these severely affected plants was taken at 60 dpi for further inoculation of a set of potato cultivars [5]; a similar approach was used in other studies (e.g., [4]).

For this research, the sap with the PSTVd strain NicTr-3 was taken from tomato cv. Rutgers after three cycles of continuous propagation over nine months and used for inoculation of potato cv. Colomba. Accumulation of viroid RNA in potato leaves was assessed at 14 and 30 dpi (Figure S3).

Unlike the potato plants infected with the original NicTr-3 strain [5], we observed no visible symptoms characteristic of disease in either the folia part or tubers of the infected plants (Figure S4). Moreover, no visible disease symptoms were recorded during the second vegetative generation derived from tubers of the infected plants. The only characteristic features of infected plants were a smaller tuber weight (Figure 2) and considerably delayed senescence: at 90 dpi, the weight of the haulm of PSTVd-infected plants was 1.6 times greater than that of the mock-inoculated plants. They also remained green, whereas the control plants underwent desiccation and senescence (Table S2). The second generation of tuber-derived plantlets was undistinguishable from the control.

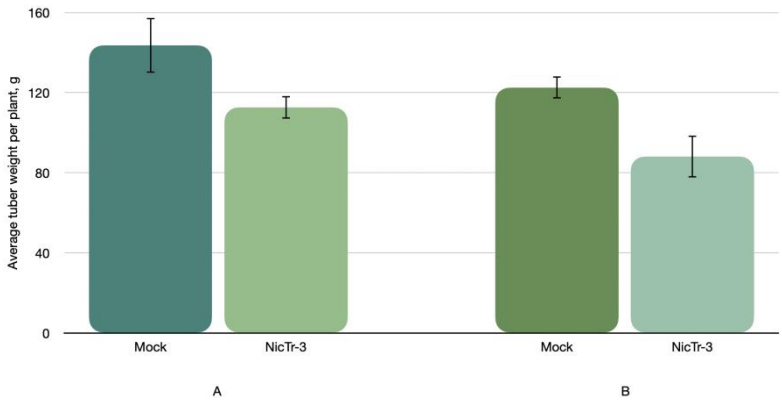

Figure 2. Average tuber weight (g) per plant inoculated with the PSTVd strain NicTr-3 and mock-inoculated plants of cv. Colomba: (**A**)—after the first inoculation, (**B**)—tubers of the second generation obtained from PSTVd-infected plants.

3.2. Nucleotide Sequence of the PSTVd Strain NicTr-3 Variants Isolated from Tomato Sap

Nucleotide sequences of viroid RNA in nine cloned variants were compared with the reference sequence of the NicTr-3 strain (Genbank LC654171) used for the first tomato passage. Mutations were classified according to their localizations in the viroid domains (TL (1–46, 316–359), P (46–74, 241–288), C (74–120, 288–316), V (120–140, 212–241), and TR (140–212)). It was found that each clone contained three to five mutations (Table S3, see also [25]). One may see that some positions were more frequently mutated (67, 120, 309), and position 67 belongs to the P (pathogenicity) domain. It seems likely that the observed attenuation of the disease symptoms of potato cv. Colomba may result from the changes in strain NicTr-3 genomic RNA accumulated during long-lasting persistence in the tomato host.

3.3. Transcriptome Analysis

Fifteen libraries of paired-end short reads were analyzed. Raw sizes of mRNA libraries varied from 55.6 million reads to 78.8 million reads (64.7 million on average). After filtering, on average 1.82% of reads were removed. Dart software successfully mapped 94% of clean library reads to the reference genome (Table S4).

Based on the expression matrix obtained with the featureCounts software, 15,788 from 39,021 potato genes annotated in *S. tuberosum* genome were removed from further analysis as having expression levels below the significance threshold. Expression levels of the remaining 23,233 genes were used to perform sample clustering. The distribution of mRNA-seq libraries is shown in Figure 3 (an outlier library S2 (red circle in the upper right corner) was removed from further analysis).

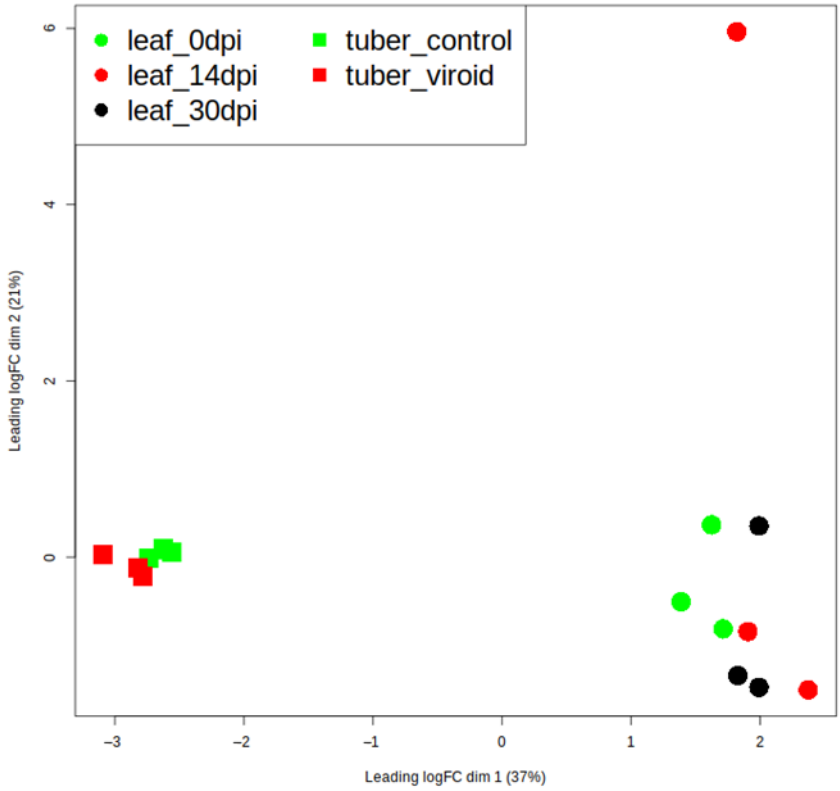

Figure 3. Clustering of mRNA-seq libraries with multidimensional scaling.

Differential expression analysis failed to identify any significant DEGs between viroid-inoculated and control samples of tuber-derived plantlets. Transcriptomes from the leaves of PSTVd-infected plants revealed the most pronounced difference between the samples from 30 dpi and 0 dpi time points. Table 1 shows the numbers of differentially expressed genes in three performed comparisons. Expression levels change values and significance levels are shown in Table S5.

Table 1. Numbers of differentially expressed genes in the leave transcriptomes.

Comparison	Number of DEGs	
	Upregulated	Downregulated
14 dpi versus 0 dpi	101	8
30 dpi versus 14 dpi	107	506
30 dpi versus 0 dpi	1909	2660

3.4. Gene Ontology Enrichment Analysis of Differentially Expressed Genes

Gene ontology terms enrichment analysis revealed GO terms associated with genes differentially expressed between different time points. In total, 1 GO term (Protein binding, GO:0005515, 15 DEGs, FDR = 5.1×10^{-6}) was associated with genes differentially expressed between 14 dpi and 0 dpi time points. 30 GO terms were significantly enriched for DEGs between 30 dpi and 14 dpi. In consistency with the largest number of DEGs, comparison of 30 dpi and 0 dpi time points yielded the largest number of enriched GO terms; 40 and 76 GO terms were associated with genes up- and down-regulated at 30 dpi, respectively (Table 2). The full lists of encountered GO terms is available in Table S6.

Table 2. Numbers of GO terms significantly enriched for lists of up- and down-regulated DEGs in different samples comparisons.

Comparison	Upregulated	Downregulated
14 dpi vs. 0 dpi	1	0
30 dpi vs. 14 dpi	0	30
30 dpi vs. 0 dpi	40	76

Analysis of GO terms revealed a relatively small difference between leaf transcriptomes at 14 and 0 dpi; the only significant term was the upregulation of "protein binding" in the "Molecular Function" category (Table 3). The comparison of the transcriptomes at 0 dpi at 30 dpi revealed the most significant downregulated DEGs related to the processes of suppression of growth and cell division (microtubule-based processes, cell cycle processes, mitosis, DNA replication, organelle fission, etc.), as well as a decrease in general metabolism (phosphate metabolic processes, lipid biosynthesis processes, carbohydrate metabolic processes) and metabolism-related functions (protein binding, NAD or NADH binding, oxidoreductase activity, hydrolase activity, nucleoside-triphosphatase activity, coenzyme activity, etc.), and were associated with nearly all compartments (intracellular, organelle, chromosome, cell wall, etc.). Comparison of downregulated DEGs in leaves at 14 dpi and 30 dpi mostly demonstrated the same trends but expressed to a much lesser extent (Table S6).

Table 3. GO terms and their associations (see also Figures S5 and S6).

Comparison	Upregulated GO Terms and Associated Processes	Downregulated GO Terms and Associated Processes
30 dpi vs. 0 dpi	**Biological Process**: 21 significant terms, including: *Response to various stimuli and oxidation stress:* oxidation reduction, transcription, multicellular organismal process, response to external and endogenous stimulus, response to organic substances, macromolecule modification. *Metabolic processes:* phosphate metabolic process, photosynthesis	**Biological Process**: 32 significant terms, including: *Cell division and cycle-related terms*: cell cycle process *Metabolic processes*: phosphate, steroid, lipid, carbohydrate, glucan, polysaccharide, response to organic substances *Regulation and response to stimuli:* Response to endogenous stimulus and hormones, development, multicellular organismal process, macromolecule modification
	Molecular Function: 19 significant terms, including: *Binding of*: protein, polysaccharide, pattern, heme, tetrapyrrole *Activity of*: oxidoreductases, (protein)kinases and transferases Electron transporter	**Molecular Function**: 26 significant terms, including: *Binding of*: protein, NAD or NADH, carbohydrate, coenzyme, chaperone *Activity of*: motor, oxidoreductase, hydrolase, kinase and transferase
	Cellular Component: no significant terms	**Cellular Component**: 18 significant terms, including: organelle, macromolecular complex, microtubule, nucleosome, chromatin, cell wall
30 dpi vs. 14 dpi	**Biological Process**: no significant terms	**Biological Process**: 4 significant terms, including: DNA replication, lipid biosynthesis process, oxidation reduction, microtubule-based process
	Molecular Function: no significant terms	**Molecular Function**: 14 significant terms, including: *Binding of*: protein, NAD or NADH, copper ion *Activity of*: oxidoreductase, catalytic, hydrolase, transferase, protein kinase
	Cellular Component: no significant terms	**Cellular Component**: 12 significant terms, including: Chromosome, cytoskeleton, organelle

Upregulated DEGs (30 dpi versus 0 dpi) showed changes in a variety of biological processes (including increase in oxidation reduction, upregulation of transcription, response to external and endogenous stimuli, phosphate metabolic process, macromolecule modification) and some GO terms related to molecular functions (protein binding, oxidoreductase activity, protein kinase activity, carbohydrate binding, disulfide oxidoreductase activity). Interestingly, no significant enrichment of GO terms was found for comparison of upregulated DEGs at 30 dpi and 14 dpi. It is likely that the main effect of viroid infection in this case concerned the reduction in growth and metabolic functions (Table 3; visualization of up- and down-regulated GO terms is also shown in Figures S5 and S6).

We looked through the lists of most significant up- and downregulated DEGs between the non-infected and the viroid-infected leaves at 30 dpi. Ten genes with the most significant up- and downregulated expression levels are listed in Table 4.

Table 4. Genes with the most significant difference in expression levels in potato leaves before inoculation (0 dpi) and at 30 dpi.

	Gene	Description	logFC	FDR
		Upregulated		
1	PGSC0003DMG400004312	9-cis-epoxycarotenoid dioxygenase	4.82	0.000611605
2	PGSC0003DMG400004081	Agamous-like MADS-box protein AGL8 homolog	10.30	0.000611605
3	PGSC0003DMG400013680	Pectinesterase	4.51	0.001384518
4	PGSC0003DMG400015755	DnaJ isoform	3.97	0.001717415
5	PGSC0003DMG400001969	Carotenoid cleavage dioxygenase 4	4.69	0.001914105
		Downregulated		
1	PGSC0003DMG400037894	Aspartic proteinase nepenthesin-1	−4.72	0.001717415
2	PGSC0003DMG400020481	14 kDa proline-rich protein DC2,15	−12.28	0.001914105
3	PGSC0003DMG400025030	Receptor kinase THESEUS 1	−3.52	0.001914105
4	PGSC0003DMG400023361	Methylenetetrahydrofolate reductase	−4.65	0.001914105
5	PGSC0003DMG401014997	Zinc finger protein	−4.90	0.001914105

logFC, logarithm to base 2 of the expression fold change; FDR, false discovery rate.

The number of DEGs in the leaves of viroid-infected plants at 30 dpi is rather large, which reflects a considerable transcriptome reprogramming and changes in metabolism. GO terms enrichment analysis revealed a decrease in the expression of cell division- and growth-related genes. Viroids are not a typical pathogen with clear PAMPs and corresponding host receptors; conversely, their effects may result from occasional interaction with cellular processes, for example, through RNA-interference and downregulation of target host genes or interaction with host proteins. Interestingly, the difference between the weights of tubers and haulms of infected and healthy plants was rather small (Table S2). This could reflect the transient character of growth suppression (transcriptome changes were analyzed at 14 and 30 dpi, whereas plants characteristics were measured at 90 dpi).

It looks likely that viroid-infected potato plants in our experiments demonstrated changes in gene expression patterns corresponding to some kind of dysregulated response to abiotic stress and/or initiation of transient dormancy. Dormancy is a complex process keeping meristematic activity repressed. The GO enriched terms for downregulated DEGs mostly corresponded to inhibition of cell division and decrease in activity of metabolic processes (Table 3). The description of some DEGs and related processes is given below (the lists of up- and downregulated genes are available in Table S5).

3.5. DEGs Description

DEGs characteristic for the dormant phenotype. In addition to downregulation of many cell-cycle-related genes (Table S5), there are several markers characteristic for dormancy and its termination (for more detail, see [26]). Exit from a dormant state is accompanied by a decrease in transcription of AGAMOUS-like MADS-box transcription factor. The viroid-infected potato leaves were characterized by a strong increase in Agamous-like MADS-box protein AGL8 homolog at 14 dpi and a further increase at 30 dpi (Table S5). It was found that the expression of deoxyuridine triphosphatase (dUTPase) increases in potato just prior to sprouting [27]. Two dUTPase entries in the DEGs list were downregulated at 14 dpi and (more strongly) at 30 dpi. The cell-wall-modifying enzymes are also involved in dormancy release. Xyloglucan endotransglucosylase (XTN) is associated with cell wall loosening [28] needed for cell division and growth. Thirteen out of sixteen XTN DEGs with significantly changed expression levels were downregulated at 30 dpi, which may also be associated with ABA synthesis [29]. In addition, eight entries for glycosyltransferases and twelve entries for polygalacturonases were significantly downregulated, which may also reflect cell division delay and growth retardation.

Two entries in the DEGs list encoding auxin-repressed/dormancy-associated protein were strongly upregulated at 30 dpi. This protein functions as an inhibitor of auxin accumulation and its overexpression results in smaller growth and yield [30,31]. The 14 kDa proline-rich protein DC2,15 is strongly suppressed in viroid-infected plants at 30 dpi. This protein is involved in cell wall modification and may be connected with the initiation of organogenesis by the removal of auxin [32].

ABA regulatory pathway. The initiation and maintenance of dormancy is associated with ABA, and the release from the dormant state is regulated by an increase in both cytokinin and gibberellin contents [26]. The list of significantly upregulated genes starts from 9-cis-epoxycarotenoid dioxygenase (NCED, a rate-limiting enzyme in abscisic acid (ABA) biosynthesis; all three entries in the DEGs list were significantly and increasingly upregulated at 14 and 30 dpi) (Table S5). Two out of three transcripts encoding ABA receptor PYL4 were strongly upregulated. The ABA regulatory pathway also involves a protein phosphatase 2c (PP2C) as a negative regulator; five entries of PP2C in the DEGs list were significantly downregulated at 30 dpi.

Expression of all four genes encoding receptor kinase THESEUS 1 was significantly repressed at 30 dpi. This transmembrane receptor-like kinase is a cell wall integrity sensor [33] involved in lateral root initiation, root skewing under salt stress, and pathogen response [34]. THE1 interacts with a signaling peptide RALF34 and is required for hypocotyl cell elongation and responses to cell wall damage. Interestingly, THE1 acts as a negative regulator of ABA-mediated root growth inhibition [33], and decrease in its transcription in viroid-infected plants may also be associated with the observed transient growth retardation phenotype.

Notably, an increased level of ABA biosynthesis enzymes did not result in a large-scale transcriptome reprogramming typical of plant response to abiotic stresses. For example, all four entries for ABA-dependent dehydration-specific RD22 genes [35] in the DEGs list were significantly downregulated despite the simultaneous increase in NCED transcription, no increase in Delta 1-pyrroline-5-carboxylate synthetase transcription was detected, etc.

DEGs characteristic of other phytohormones metabolic pathways. Transcription of three Cytokinin oxidase/dehydrogenase (CKX) transcripts was significantly increased at 30 dpi. This enzyme plays a key role in regulating cytokinin levels in plants by degrading its excess [36]. Since elevations of both cytokinin and gibberellin contents are associated with the dormancy release [26], the observed increase in CKX transcription may accompany the transition of infected potato to a dormant state.

Five entries encoding 1-aminocyclopropane-1-carboxylate oxidase (ACO) were upregulated at 30 dpi whereas no increase in 1-aminocyclopropane-1-carboxylate synthase (ACS) and a significant decrease in S-adenosylmethionine synthase were observed. Interestingly, in grapevine, the level of ACO transcription sharply decreases during natural dormancy release [37]. It has been reported that ABA could regulate climacteric fruit ripening by

inducing ethylene production [38]; thus, some interconnections are possible. In general, overproduction of ethylene results in plant growth reduction [39].

In the gibberellin biosynthesis pathway, a significant increase in expression of Ga20 oxidases (three out of four entries in the DEGs list) and GID1-like gibberellin receptors (four entries in the DEGs list) was detected, whereas transcription of a negative GA regulator Gibberellin 2-oxidase (three out of four entries in the DEGs list) was downregulated, which may reflect its activation. However, expression of Della, Ent-kaurenoic acid oxidase, and Ent-kaurene oxidase was generally decreased (Table S5). In potato, ABA and GA play antagonistic roles in the development of the stem and tubers: GA promotes stem growth and represses tuber swelling, whereas ABA stimulates tuber formation [40].

Five entries of CONSTANS transcription factor regulating flowering and promoting tuberization [41], Flowering locus T (two entries of three), and two entries for Bel5 protein were strongly upregulated. All these genes are involved in induction of tuberization [42].

Comparison with other viroid-related transcriptomic data. Transcriptome investigations provide a large amount of data for reconstruction of molecular mechanisms involved in response to viroid infection despite an observed considerable diversity and specificity in viroid-host interactions [43–45].

The transcriptome investigations of mild and severe variants of PSTVd have been performed on tomato. Więsyk et al. [43] analyzed early response in tomato and found 933 and 2731 significant DEGs in mild and severe viroid-infected variants at 17 dpi, respectively, with only 418 common DEGs. Similar to our results, the downregulated DEGs were enriched in terms corresponding to the cell cycle and microtubules, as well as to photosynthesis. The revealed DEGs reflect activation of defense response and an elevated level of SA and PR1 protein (e.g., [46]). In our research, the list of significantly upregulated DEGs includes transcripts encoding PR1 protein and two pathogenesis-induced proteins. However, entries for many other pathogenesis-related proteins were not significantly upregulated (e.g., chitinases, PR10), which may reflect the absence of a systemic response.

The detailed analysis of up- and downregulated DEGs at 17, 24, and 49 dpi was published for tomato infected with mild and severe strains of PSTVd [47]. Despite noticeable similarity, some major features of hormone metabolism-related DEGs in our experiments were rather different, namely, no significant increase in ABA biosynthesis-related genes was detected in their research.

Fujinayashi et al. [11] proposed that the severe PSTVd symptoms correlated with ROS production and downregulation of ROS-scavenging enzymes. In tomato cv. Moneymaker, PSTVd infection was nearly asymptomatic and SOD genes were upregulated, whereas strongly affected cv. Rutgers was characterized by suppression of Cu/Zn-SOD genes via PSTVd-induced overexpression of miR398 and miR398a-3, respectively. In our research, we observed some decrease in two out of three Cu/Zn-SOD transcripts, and some increase in one out of four Mn/Fe-SOD transcripts.

4. Conclusions

1. The PSTVd strain NicTr-3 found in severely affected potato plants of cv. Nikulinskiy was characterized with a high aggressiveness against tomato cv. Rutgers and potato cv. Colomba [5]. However, after three cycles of propagation in tomato cv. Rutgers it became attenuated against potato cv. Colomba and resulted in a statistically significant decrease in tuber weight and a considerable delay of leaf senescence. It was found that the viroid RNAs in tomato sap contained a number of mutated variants that may be connected with the observed attenuation.
2. Analysis of transcriptomes from PSTVd-inoculated potato leaves revealed a significant difference with control cv. Colomba plants. Interestingly, no significant difference was detected between the transcriptomes of the tuber-derived plantlets representing the second vegetative generation. The transcriptome comparison revealed the signs of dysregulation of signal transduction pathways resembling the initiation of dormancy and transient growth delay. It involves the upregulation of

9-cis-epoxycarotenoid dioxygenase gene encoding a rate-limiting enzyme of ABA biosynthesis, induction of AGAMOUS-like MADS-box transcription factor, auxin-repressed/dormancy-associated protein, repression of cytokinin-degrading enzymes, upregulation of tuberization factors CONSTANS, Flowering locus T, Bel5, and so on. The connection between the attenuated viroid strain and the observed changes in potato leaf transcriptomes remains obscure. It is likely that the considerable delay in leaf senescence (Table S2) resulted from this transcriptome dysregulation [48].

3. Taking into account the relatively small changes in phenotype and no significant difference being found between the transcriptomes of the second vegetative generation and the non-infected potato plants, the search for potential vaccine-like viroid variants may represent one of possible ways for biocontrol of these harmful pathogenic RNAs. Indeed, there are many threats and obstacles accompanying the development of such technologies, but this way seems to be worth the effort.

Supplementary Materials: The following are available online at https://www.mdpi.com/article/10.3390/agronomy13030684/s1, Table S1: The description of gene-specific primers used for cDNA (qRT-PCR) amplifications; Table S2: Tubers and haulm weight at 90 dpi with PSTVd strain NicTr-3; Table S3: Heterogeneity of variants of the potato spindle tuber viroid strain NicTr-3; Table S4: Libraries characteristics; Table S5. DEGs characteristics; Table S6. GO enriched terms. Figure S1: Verification of significant difference of DEGs by qPCR; Figure S2. Symptoms of plants of cv. Colomba infected with original PSTVd strain NicTr-3; Figure S3. RT-PCR detection of PSTVd in potato leaves of cv. Colomba; Figure S4. Tubers of potato plants of cv. Colomba after inoculation with PSTVd-infected (strain NicTr-3) tomato sap; Figure S5: Visualization of AgriGO2 (30 dpi vs. 0 dpi); Figure S6: Visualization of AgriGO2 (30 dpi vs. 14 dpi).

Author Contributions: Conceptualization, A.V.K. (Alex V. Kochetov), O.S.A.; Methodology, G.V.V., N.V.S., N.V.M., N.M.L., Software, D.A.A., N.S.; Validation, A.A.E.; Investigation, A.V.K. (Alexander V. Khiutti), O.S.A., A.V.K. (Alex V. Kochetov), N.V.M.; Writing A.V.K. (Alexander V. Khiutti), O.S.A.; Project Administration, A.V.K. (Alexander V. Khiutti), O.S.A. All authors have read and agreed to the published version of the manuscript.

Funding: The research was supported by the Russian Science Foundation (RSF) No. 20-46-07001. Bioinformatic analysis was supported by Kurchatov Genomics Center of IC&G (No. 075–15–2019-1662). NGS sequencing was conducted in the ICG Joint Center for Genome Studies (supported in the frame of ICG budget project No. FWNR-2022-0017).

Data Availability Statement: Raw sequencing data are deposited in NCBI Sequence Read Archive (PRJNA914898).

Conflicts of Interest: The authors declare no conflict of interest.

References

1. Diener, T.O. The viroid: Biological oddity or evolutionary fossil? *Adv. Virus Res.* **2001**, *57*, 137–184. [CrossRef] [PubMed]
2. Mackie, A.E.; Rodoni, B.C.; Barbetti, M.J.; McKirdy, S.J.; Jones, R.A.C. Potato spindle tuber viroid: Alternative host reservoirs and strain found in a remote subtropical irrigation area. *Eur. J. Plant Pathol.* **2016**, *145*, 433–446. [CrossRef]
3. EPPO. National regulatory control systems: Potato spindle tuber viroid on potato. *EPPO Bull.* **2011**, *41*, 394–399. [CrossRef]
4. Mackie, A.E.; Barbetti, M.J.; Rodoni, B.; McKirdy, S.J.; Jones, R.A.C. Effects of a Potato Spindle Tuber Viroid Tomato Strain on the Symptoms, Biomass, and Yields of Classical Indicator and Currently Grown Potato and Tomato Cultivars. *Plant Dis.* **2019**, *103*, 3009–3017. [CrossRef]
5. Afanasenko, O.S.; Lashina, N.M.; Mironenko, N.V.; Kyrova, E.I.; Rogozina, E.V.; Zubko, N.G.; Khiutti, A.V. Evaluation of Responses of Potato Cultivars to Potato Spindle Tuber Viroid and to Mixed Viroid/Viral Infection. *Agronomy* **2022**, *12*, 2916. [CrossRef]
6. Fernow, K.H. Tomato as a test plant for detecting mild strains of potato spindle tuber virus. *Phytopathology* **1967**, *57*, 1347–1352.
7. Matsushita, Y.; Yanagisawa, H.; Khiutti, A.; Mironenko, N.; Ohto, Y.; Afanasenko, O. Genetic diversity and pathogenicity of potato spindle tuber viroid and chrysanthemum stunt viroid isolates in Russia. *Eur. J. Plant Pathol.* **2021**, *161*, 529–542. [CrossRef]
8. Aviña-Padilla, K.; Zambada-Moreno, O.; Herrera-Oropeza, G.E.; Jimenez-Limas, M.A.; Abrahamian, P.; Hammond, R.W.; Hernández-Rosales, M. Insights into the Transcriptional Reprogramming in Tomato Response to PSTVd Variants Using Network Approaches. *Int. J. Mol. Sci.* **2022**, *23*, 5983. [CrossRef]

9. Kitabayashi, S.; Tsushima, D.; Adkar-Purushothama, C.; Sano, T. Identification and Molecular Mechanisms of Key Nucleotides Causing Attenuation in Pathogenicity of Dahlia Isolate of Potato Spindle Tuber Viroid. *Int. J. Mol. Sci.* **2020**, *21*, 7352. [CrossRef]
10. Adkar-Purushothama, C.R.; Bolduc, F.; Bru, P.; Perreault, J.-P. Insights into Potato Spindle Tuber Viroid Quasi-Species from Infection to Disease. *Front. Microbiol.* **2020**, *11*, 1235. [CrossRef]
11. Fujibayashi, M.; Suzuki, T.; Sano, T. Mechanism underlying potato spindle tuber viroid affecting tomato (*Solanum lycopersicum*): Loss of control over reactive oxygen species production. *J. Gen. Plant Pathol.* **2021**, *87*, 226–235. [CrossRef]
12. Naoi, T.; Hataya, T. Tolerance Even to Lethal Strain of Potato Spindle Tuber Viroid Found in Wild Tomato Species Can Be Introduced by Crossing. *Plants* **2021**, *10*, 575. [CrossRef]
13. Adkar-Purushothama, C.R.; Perreault, J.-P. Alterations of the viroid regions that interact with the host defense genes attenuate viroid infection in host plant. *RNA Biol.* **2018**, *15*, 955–966. [CrossRef]
14. Bao, S.; Owens, R.A.; Sun, Q.; Song, H.; Liu, Y.; Eamens, A.L.; Feng, H.; Tian, H.; Wang, M.-B.; Zhang, R. Silencing of transcription factor encoding gene *StTCP23* by small RNAs derived from the virulence modulating region of potato spindle tuber viroid is associated with symptom development in potato. *PLOS Pathog.* **2019**, *15*, e1008110. [CrossRef]
15. Cisneros, A.E.; Lisón, P.; Campos, L.; López-Tubau, J.M.; Altabella, T.; Ferrer, A.; Daròs, J.-A.; Carbonell, A. Down-regulation of tomato STEROL GLYCOSYLTRANSFERASE 1 perturbs plant development and facilitates viroid infection. *J. Exp. Bot.* **2022**, erac361. [CrossRef]
16. Prol, F.V.; López-Gresa, M.P.; Rodrigo, I.; Bellés, J.M.; Lisón, P. Ethylene is Involved in Symptom Development and Ribosomal Stress of Tomato Plants upon Citrus Exocortis Viroid Infection. *Plants* **2020**, *9*, 582. [CrossRef]
17. Navarro, B.; Gisel, A.; Serra, P.; Chiumenti, M.; Di Serio, F.; Flores, R. Degradome Analysis of Tomato and *Nicotiana benthamiana* Plants Infected with Potato Spindle Tuber Viroid. *Int. J. Mol. Sci.* **2021**, *22*, 3725. [CrossRef]
18. Chen, S.; Zhou, Y.; Chen, Y.; Gu, J. fastp: An ultra-fast all-in-one FASTQ preprocessor. *Bioinformatics* **2018**, *34*, i884–i890. [CrossRef]
19. The Potato Genome Sequencing Consortium. Genome sequence and analysis of the tuber crop potato. *Nature* **2011**, *475*, 189–195. [CrossRef]
20. Yates, A.D.; Allen, J.; Amode, R.M.; Azov, A.G.; Barba, M.; Becerra, A.; Bhai, J.; Campbell, L.I.; Martinez, M.C.; Chakiachvili, M.; et al. Ensembl Genomes 2022: An expanding genome resource for non-vertebrates. *Nucleic Acids Res.* **2022**, *50*, D996–D1003. [CrossRef]
21. Lin, H.-N.; Hsu, W.-L. DART: A fast and accurate RNA-seq mapper with a partitioning strategy. *Bioinformatics* **2018**, *34*, 190–197. [CrossRef]
22. Liao, Y.; Smyth, G.K.; Shi, W. The R package Rsubread is easier, faster, cheaper and better for alignment and quantification of RNA sequencing reads. *Nucleic Acids Res.* **2019**, *47*, e47. [CrossRef]
23. Robinson, M.D.; McCarthy, D.J.; Smyth, G.K. EdgeR: A Bioconductor package for differential expression analysis of digital gene expression data. *Bioinformatics* **2010**, *26*, 139–140. [CrossRef]
24. Tian, T.; Liu, Y.; Yan, H.; You, Q.; Yi, X.; Du, Z.; Xu, W.; Su, Z. agriGO v2.0: A GO analysis toolkit for the agricultural community, 2017 update. *Nucleic Acids Res.* **2017**, *45*, W122–W129. [CrossRef]
25. Mironenko, N.V.; Orina, A.S.; Lashina, N.M.; Afanasenko, O.S. Expression of transcription factor encoding *StTCP23* gene in potato plants infected with tuber spindle viroid. *Proc. Appl. Bot. Genet. Breed* 2023, *184*, in press.
26. Campbell, M.; Suttle, J.; Douches, D.S.; Buell, C.R. Treatment of potato tubers with the synthetic cytokinin 1-(α-ethylbenzyl)-3-nitroguanidine results in rapid termination of endodormancy and induction of transcripts associated with cell proliferation and growth. *Funct. Integr. Genom.* **2014**, *14*, 789–799. [CrossRef]
27. Senning, M.; Sonnewald, U.; Sonnewald, S. Deoxyuridine triphosphatase expression defines the transition from dormant to sprouting potato tuber buds. *Mol. Breed.* **2010**, *26*, 525–531. [CrossRef]
28. Van Sandt, V.S.T.; Suslov, D.; Verbelen, J.-P.; Vissenberg, K. Xyloglucan Endotransglucosylase Activity Loosens a Plant Cell Wall. *Ann. Bot.* **2007**, *100*, 1467–1473. [CrossRef]
29. Gimeno-Gilles, C.; Lelièvre, E.; Viau, L.; Malik-Ghulam, M.; Ricoult, C.; Niebel, A.; Leduc, N.; Limami, A.M. ABA-Mediated Inhibition of Germination Is Related to the Inhibition of Genes Encoding Cell-Wall Biosynthetic and Architecture: Modifying Enzymes and Structural Proteins in Medicago truncatula Embryo Axis. *Mol. Plant* **2009**, *2*, 108–119. [CrossRef]
30. Zhao, Y.; Li, C.; Ge, J.; Xu, M.; Zhu, Q.; Wu, T.; Guo, A.; Xie, J.; Dong, H. Recessive Mutation Identifies Auxin-Repressed Protein ARP1, Which Regulates Growth and Disease Resistance in Tobacco. *Mol. Plant Microbe Interact.* **2014**, *27*, 638–654. [CrossRef]
31. De Souza, G.B.; Mendes, T.A.D.O.; Fontes, P.P.; Barros, V.D.A.; Gonçalves, A.B.; Ferreira, T.D.F.; Costa, M.D.-B.L.; Alves, M.S.; Fietto, L.G. Genome-wide identification and expression analysis of dormancy-associated gene 1/auxin repressed protein (DRM1/ARP) gene family in Glycine max. *Prog. Biophys. Mol. Biol.* **2019**, *146*, 134–141. [CrossRef]
32. Aleith, F.; Richter, G. Gene expression during induction of somatic embryogenesis in carrot cell suspensions. *Planta* **1991**, *183*, 17–24. [CrossRef]
33. Bacete, L.; Schulz, J.; Engelsdorf, T.; Bartosova, Z.; Vaahtera, L.; Yan, G.; Gerhold, J.M.; Tichá, T.; Øvstebø, C.; Gigli-Bisceglia, N.; et al. THESEUS1 modulates cell wall stiffness and abscisic acid production in *Arabidopsis thaliana*. *Proc. Natl. Acad. Sci. USA* **2022**, *119*, e2119258119. [CrossRef]
34. Gorgues, L.; Li, X.; Maurel, C.; Martinière, A.; Nacry, P. Root osmotic sensing from local perception to systemic responses. *Stress Biol.* **2022**, *2*, 36. [CrossRef]

35. Hussain, Q.; Asim, M.; Zhang, R.; Khan, R.; Farooq, S.; Wu, J. Transcription Factors Interact with ABA through Gene Expression and Signaling Pathways to Mitigate Drought and Salinity Stress. *Biomolecules* **2021**, *11*, 1159. [CrossRef]
36. Blume, R.; Yemets, A.; Korkhovyi, V.; Radchuk, V.; Rakhmetov, D.; Blume, Y. Genome-wide identification and analysis of the cytokinin oxidase/dehydrogenase (ckx) gene family in finger millet (*Eleusine coracana*). *Front. Genet.* **2022**, *13*, 963789. [CrossRef]
37. Shi, Z.; Halaly-Basha, T.; Zheng, C.; Weissberg, M.; Ophir, R.; Galbraith, D.W.; Pang, X.; Or, E. Transient induction of a subset of ethylene biosynthesis genes is potentially involved in regulation of grapevine bud dormancy release. *Plant Mol. Biol.* **2018**, *98*, 507–523. [CrossRef]
38. Mou, W.; Li, D.; Luo, Z.; Li, L.; Mao, L.; Ying, T. SlAREB1 transcriptional activation of NOR is involved in abscisic acid-modulated ethylene biosynthesis during tomato fruit ripening. *Plant Sci.* **2018**, *276*, 239–249. [CrossRef]
39. Dubois, M.; Van den Broeck, L.; Inzé, D. The Pivotal Role of Ethylene in Plant Growth. *Trends Plant Sci.* **2018**, *23*, 311–323. [CrossRef]
40. Chen, P.; Yang, R.; Bartels, D.; Dong, T.; Duan, H. Roles of Abscisic Acid and Gibberellins in Stem/Root Tuber Development. *Int. J. Mol. Sci.* **2022**, *23*, 4955. [CrossRef]
41. Cao, D.; Lin, Z.; Huang, L.; Damaris, R.N.; Li, M.; Yang, P. A CONSTANS-LIKE gene of Nelumbo nucifera could promote potato tuberization. *Planta* **2021**, *253*, 65. [CrossRef]
42. Navarro, C.; Cruz-Oró, E.; Prat, S. Conserved function of FLOWERING LOCUS T (FT) homologues as signals for storage organ differentiation. *Curr. Opin. Plant Biol.* **2015**, *23*, 45–53. [CrossRef]
43. Więsyk, A.; Lirski, M.; Fogtman, A.; Zagórski-Ostoja, W.; Góra-Sochacka, A. Differences in gene expression profiles at the early stage of *Solanum lycopersicum* infection with mild and severe variants of potato spindle tuber viroid. *Virus Res.* **2020**, *286*, 198090. [CrossRef]
44. Joubert, M.; Berg, N.V.D.; Theron, J.; Swart, V. Transcriptomics Advancement in the Complex Response of Plants to Viroid Infection. *Int. J. Mol. Sci.* **2022**, *23*, 7677. [CrossRef]
45. Chi, S.; Zhang, J.; Li, H.; Wang, P.; Feng, L.; Ren, Y. RNA-seq Profiling Reveals the Transcriptional Response Against Potato Spindle Tuber Viroid in Different Potato Cultivars and Developmental Stages. *Potato Res.* **2022**, *65*, 979–990. [CrossRef]
46. Prol, F.V.; Márquez-Molins, J.; Rodrigo, I.; López-Gresa, M.; Bellés, J.; Gómez, G.; Pallás, V.; Lisón, P. Symptom Severity, Infection Progression and Plant Responses in Solanum Plants Caused by Three Pospiviroids Vary with the Inoculation Procedure. *Int. J. Mol. Sci.* **2021**, *22*, 6189. [CrossRef]
47. Góra-Sochacka, A.; Więsyk, A.; Fogtman, A.; Lirski, M.; Zagórski-Ostoja, W. Root Transcriptomic Analysis Reveals Global Changes Induced by Systemic Infection of Solanum lycopersicum with Mild and Severe Variants of Potato Spindle Tuber Viroid. *Viruses* **2019**, *11*, 992. [CrossRef]
48. Zhao, Y.; Gao, J.; Kim, J.I.; Chen, K.; Bressan, R.A.; Zhu, J.-K. Control of Plant Water Use by ABA Induction of Senescence and Dormancy: An Overlooked Lesson from Evolution. *Plant Cell Physiol.* **2017**, *58*, 1319–1327. [CrossRef]